

# Direct Evidence of Active-Site Reduction and Photodriven Catalysis in Sensitized Hydrogenase Assemblies

Brandon L. Greene,<sup>†</sup> Crisjoe A. Joseph,<sup>‡</sup> Michael J. Maroney,<sup>‡</sup> and R. Brian Dyer<sup>\*†</sup>

<sup>†</sup>Chemistry Department, Emory University, Atlanta, Georgia 30322, United States

<sup>‡</sup>Chemistry Department, University of Massachusetts Amherst, Amherst, Massachusetts 01003, United States

**S** Supporting Information

**ABSTRACT:** We report photocatalytic H<sub>2</sub> production by hydrogenase (H<sub>2</sub>ase)–quantum dot (QD) hybrid assemblies. Quenching of the CdTe exciton emission was observed, consistent with electron transfer from the quantum dot to H<sub>2</sub>ase. GC analysis showed light-driven H<sub>2</sub> production in the presence of a sacrificial electron donor with an efficiency of 4%, which is likely a lower limit for these hybrid systems. FTIR spectroscopy was employed for direct observation of active-site reduction in unprecedented detail for photodriven H<sub>2</sub>ase catalysis with sensitivity toward both H<sub>2</sub>ase and the sacrificial electron donor. Photosensitization with Ru(bpy)<sub>3</sub><sup>2+</sup> showed distinct FTIR photoreduction properties, generating all of the states along the steady-state catalytic cycle with minimal H<sub>2</sub> production, indicating slow, sequential one-electron reduction steps. Comparing the H<sub>2</sub>ase activity and FTIR results for the two systems showed that QDs bind more efficiently for electron transfer and that the final enzyme state is different for the two sensitizers. The possible origins of these differences and their implications for the enzymatic mechanism are discussed.

Hydrogenases (H<sub>2</sub>ases) catalyze the two reactions that are fundamental for a viable hydrogen-based economy: the reduction of protons in water to hydrogen and the oxidation of hydrogen to protons. One class of H<sub>2</sub>ases, denoted [NiFe] on the basis of the metal content of the active site, is tolerant of or reversibly inhibited by O<sub>2</sub>, and consequentially, it has been heavily studied for biotechnology applications.<sup>1–5</sup> Recent research has explored the use of light to drive the chemistry of H<sub>2</sub>ase enzymes with a variety of photosensitizers, including photosystem I, ruthenium-sensitized TiO<sub>2</sub>, and quantum dots (QDs).<sup>6–12</sup> Light-induced H<sub>2</sub> generation and electron transfer (ET) have been characterized, but no one to date has used this approach for rapid initiation of turnover for mechanistic studies. Triggering enzyme turnover with light may provide exquisite control of the complex catalytic cycle [Figure SI-1 in the Supporting Information (SI)], which may enable the direct observation of short-lived intermediates by IR spectroscopy through the CO and CN<sup>−</sup> ligands bound to iron in the active site.

Herein we present a hybrid photocatalyst that couples H<sub>2</sub>ase from *Thiocapsa roseopersicina* (*Tr*) and mercaptopropionic acid (MPA)-capped CdTe QDs for efficient visible-light-driven

hydrogen production. This [NiFe] H<sub>2</sub>ase was selected for its overall chemical stability toward various buffers, pH, and ionic strength as well as its exceptional thermal stability, high tolerance toward O<sub>2</sub>, and reversible reactivation.<sup>4</sup> FTIR spectroscopy provided direct evidence of active-site reduction as well as sacrificial electron donor (SED) consumption, and GC analysis confirmed highly efficient enzyme turnover. Comparison with Ru(bpy)<sub>3</sub><sup>2+</sup>-sensitized H<sub>2</sub>ase revealed striking differences that we attribute in part to the efficiency of photoreduction, which may have important implications for the catalytic mechanism.

Understanding the interaction between the QD and enzyme surface is of critical importance for the design of ET-active binding.<sup>13</sup> Electrostatic binding was used as the simplest approach to attach the QD photosensitizer to the enzyme. Since the crystal structure of the *Tr* H<sub>2</sub>ase has not been determined, homology modeling (Figure SI-2) was performed to assess possible binding sites of the CdTe QD.<sup>14,15</sup> The model shows a positively charged region around the small subunit near the distal and medial FeS clusters. We hypothesize this region to be the most likely binding site for the negatively charged CdTe QD. Binding at this site should orient the QD optimally on the enzyme surface for interfacial ET to the distal or medial FeS cluster.<sup>13</sup>

The QD photoluminescence quantum efficiency (PLQE) has previously been shown to be sensitive to molecules and proteins adsorbed on the QD in nanoparticle assemblies.<sup>6,16,17</sup> We used this property of QDs to investigate the nature of the H<sub>2</sub>ase–QD binding interaction and nonradiative contributions to excitonic quenching from H<sub>2</sub>ase adsorbed on the QD surface (Figure 1).

Titration of QDs with H<sub>2</sub>ase showed quenching of the PLQE. We attribute the decrease in PLQE to a nonradiative ET quenching mechanism that directly reduces the distal FeS cluster. The observed behavior is likely due to higher interfacial ET efficiency (decreases the PLQE) relative to the proposed surface passivation effect (increases the PLQE).<sup>16,17</sup> We postulate that surface passivation indeed occurs but that the high ET efficiency obscures the predicted increase in PLQE due to surface passivation. The PL quenching did not show saturation over the accessible range of H<sub>2</sub>ase concentrations, preventing detailed analysis of the binding constant and free energy, but salt screening effects (see below) corroborated the

Received: May 2, 2012

Published: June 21, 2012

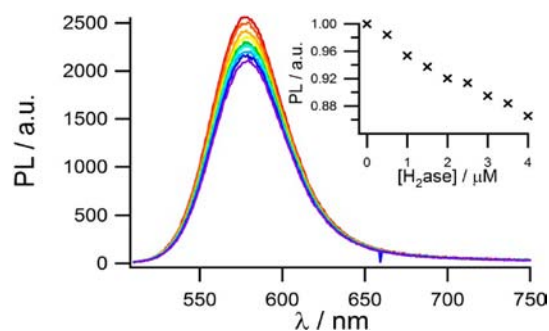


**Figure 1.** PL titration spectra of 500 nM CdTe QDs with H<sub>2</sub>ase (red, 0 μM H<sub>2</sub>ase; purple, 4 μM H<sub>2</sub>ase) in 100 mM phosphate buffer (pH 7.5). The inset shows the integrated PL intensity as a function of H<sub>2</sub>ase concentration.

electrostatic binding. The titration indicated a binding constant of  $<10^6 \text{ M}^{-1}$  (see the SI) or that the binding was not 1:1.

Encouraged by the evidence for ET in the PL titration, FTIR experiments were performed in an attempt to observe photoreduction at the active site. Light titrations monitored by FTIR difference spectroscopy were used to follow the active-site reduction through frequency shifts in the CO and CN<sup>-</sup> bands observed after enzyme reduction (Figure 2).

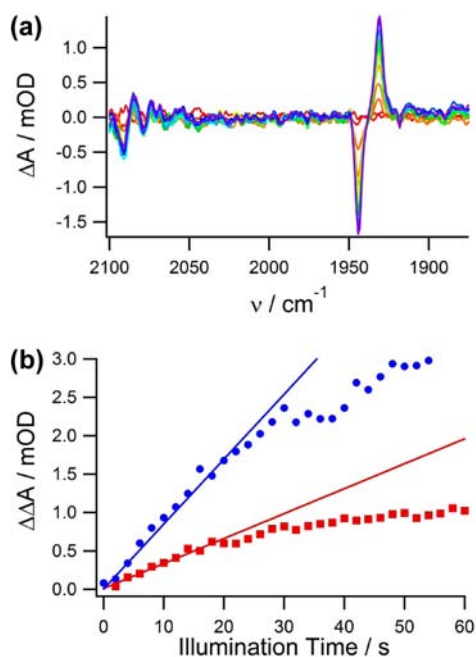


**Figure 2.** (a) Light titrations ( $\lambda = 527 \text{ nm}$ ) of 500 μM H<sub>2</sub>ase, 1 mM QDs, and 50 mM ascorbate in 100 mM phosphate buffer (pH 7.4), probed by FTIR spectroscopy. The illumination time ranged from 0 s (red) to 12.5 s (purple). (b) Comparison of peak-to-peak absorbance differences in going from ascorbate to dehydroascorbate (blue ●) and Ni<sub>i</sub>-B to Ni<sub>a</sub>-S (red ■). Linear fits of the data for 0–10 s of illumination gave slopes of  $8.5 \times 10^{-8}$  and  $3.3 \times 10^{-8}$  for ascorbate and H<sub>2</sub>ase, respectively.

Aerobic reduction by QD excitation yielded bleached bands at 2091, 2079, and 1944  $\text{cm}^{-1}$ . These frequencies are nearly identical to the CN<sup>-</sup> and CO frequencies associated with the oxidized Ni<sub>i</sub>-B state of [NiFe] from *Desulfovibrio gigas*.<sup>18</sup> Induced absorbances at 2084  $\text{cm}^{-1}$ , 2075  $\text{cm}^{-1}$  and 1930  $\text{cm}^{-1}$  also matched well with the one-electron-reduced Ni<sub>a</sub>-S state,

indicating light-initiated formation of the catalytically active state.<sup>18</sup> These difference spectra represent the first IR characterization of [NiFe] H<sub>2</sub>ase from *Tr* and verify its similarity to other well-studied [NiFe] H<sub>2</sub>ases.<sup>18–20</sup> Aerobic reduction typically results in rapid reoxidation to the Ni<sub>i</sub>-B state under electron-rich conditions.<sup>4,21,22</sup> Because of the long time scale (minutes) of the steady-state FTIR difference measurements in Figure 2a, no signal would have been observed if this were the case, since the initial and final states would have been the same. We thus conclude either that photoreduction results in rapid and complete reductive O<sub>2</sub> consumption in the experimental cell, as has been proposed by Zadvornyy et al.,<sup>11</sup> or that reoxidation is kinetically hindered. The formation of further reduced states such as Ni<sub>a</sub>-C and Ni<sub>a</sub>-SR was not observed even at a short illumination time (100 ms), as expected for multielectron reduction followed by rapid (submillisecond) H<sub>2</sub> evolution that reoxidizes the enzyme to Ni<sub>a</sub>-S faster than can be observed on the time scale of the difference FTIR method.

The consumption of the SED, ascorbate, and subsequent formation of dehydroascorbate was observed in the mid-IR by following the carbonyl modes. The observed rate of ascorbate consumption was  $\sim 3$  times the rate of H<sub>2</sub>ase reduction (Figure 2b). We conclude that the apparent single electron reduction process observed in the steady-state FTIR spectrum is actually the end product of a more complex cycle involving full reduction of Ni<sub>i</sub>-B to Ni<sub>a</sub>-SR followed by rapid H<sub>2</sub> evolution to form Ni<sub>a</sub>-S. This interpretation was corroborated by anaerobic steady-state light titrations in which the enzyme was activated under H<sub>2</sub> (Figure SI-6). In these experiments, Ni<sub>a</sub>-C was observed to bleach as a function of illumination time with concomitant re-formation of the Ni<sub>a</sub>-S state and some Ni<sub>a</sub>-SR along with SED consumption. The net result is the same as the aerobic case: multielectron reduction results in H<sub>2</sub> evolution to re-form the catalytically active oxidized state.

To determine the photocatalytic H<sub>2</sub> production efficiency, GC was used to quantify the H<sub>2</sub> production (Figure 3). Rapid

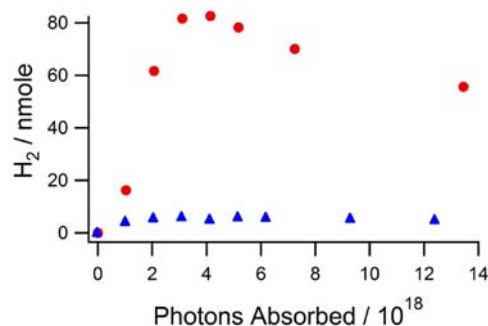


**Figure 3.** GC assay of H<sub>2</sub> production vs number of photons absorbed using 1 μM H<sub>2</sub>ase, 0.5 μM QDs, and 50 mM ascorbate at pH 7.4 in 100 mM phosphate buffer (red ●) or 50 mM TRIS-buffered seawater (blue ▲).

H<sub>2</sub> production was observed, with a peak of 81 nmol produced in 40 s of illumination. On the basis of the H<sub>2</sub> production after absorption of  $2.07 \times 10^{18}$  photons, 4% of the absorbed photons were converted to proton-reducing equivalents with an enzyme turnover number (TON) of 92 (explicit calculations of efficiency and TON are laid out in the SI). The efficiency was drastically reduced by electrostatic screening in high-ionic-strength solutions, as shown by comparison with the same

system in artificial seawater (Figure 3). This observation indicates that engineering better electrostatic interactions will likely increase the overall efficiency. Relative to similar work in the literature, our system has the disadvantage of an enzyme naturally biased toward H<sub>2</sub> oxidation but the significant advantages of O<sub>2</sub> tolerance and a better basis for mechanistic studies.<sup>23</sup> The system also shows some photodecomposition after long illumination times, as observed by Brown et al.<sup>23</sup> for similar systems, likely due to oxidation of surface ligands of the thiolate-capped QDs.

The inability to observe Ni<sub>a</sub>-C and Ni<sub>a</sub>-SR intermediates in the QD-H<sub>2</sub>ase light-initiated difference measurements means that under these conditions turnover is very efficient, consequently preventing the buildup of partially reduced intermediates. Since the instantaneous fluence and duration of the laser pulse (10 ns) were large enough to produce multiple excitation and exciton generation/dissociation events (not limited by the rate of oxidation of the SED), we postulated that multiple ET events into the protein occurred, resulting in rapid enzyme reduction and turnover. To test this hypothesis, we compared the light-driven turnover of H<sub>2</sub>ase using Ru(bpy)<sub>3</sub><sup>2+</sup>, an intrinsic single-electron photoreductant. Light titrations of Ru(bpy)<sub>3</sub><sup>2+</sup>-sensitized H<sub>2</sub>ase (Figure 4) provided

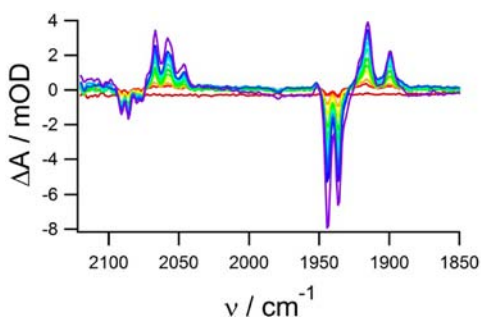


**Figure 4.** Laser-induced light titration of Ru(bpy)<sub>3</sub><sup>2+</sup>-sensitized H<sub>2</sub>ase monitored by FTIR, using 27 mM Ru(bpy)<sub>3</sub><sup>2+</sup>, 500 μM H<sub>2</sub>ase, and 100 mM ascorbate in 100 mM phosphate buffer (pD 7.4): red, dark spectrum; purple, difference FTIR spectrum after 12 s of laser illumination.

evidence for light-induced production of every known redox intermediate of the enzyme (each CO peak corresponds to a separate state). The amplitudes of the FTIR difference features increased linearly with illumination time over the entire light titration, indicating that the photoreduction rate was constant throughout the titration.

Two CO bleaches were observed, one corresponding to Ni<sub>r</sub>-B and one blue-shifted 6 cm<sup>-1</sup> from the previously observed Ni<sub>a</sub>-S state. This shift is likely due to the spectral crowding of positive features around bleaching bands, which shifts the apparent peak position away from the adjacent positive feature. Bleaching of the CN<sup>-</sup> bands assigned to Ni<sub>r</sub>-B and Ni<sub>a</sub>-S was also observed, indicating that the bleach at 1937 cm<sup>-1</sup> was in fact due to Ni<sub>a</sub>-S. Induced absorbances were observed at 1915 cm<sup>-1</sup> (Ni<sub>r</sub>-S), 1899 cm<sup>-1</sup> (Ni-L\*), and 1951 cm<sup>-1</sup> (Ni<sub>a</sub>-C), with a shoulder growing in at 1921 cm<sup>-1</sup> that is associated with the fully reduced state Ni<sub>a</sub>-SR.<sup>24,25</sup> A small amount of SED consumption was observed, confirming its involvement in the re-reduction of the Ru(bpy)<sub>3</sub><sup>3+</sup>, but the amount of ascorbate oxidation was too small to quantify by FTIR spectroscopy. Under the reaction conditions employed, the bimolecular reaction of Ru(bpy)<sub>3</sub><sup>3+</sup> with ascorbate is much faster than that

of reduction by H<sub>2</sub>O/OH<sup>-</sup> (with pseudo-first-order rate constants of 10<sup>8</sup> and 10<sup>-3</sup> s<sup>-1</sup>, respectively).<sup>26,27</sup> Regeneration of Ru(bpy)<sub>3</sub><sup>2+</sup> may occur on a fast time scale, but because of the lower binding affinity or lower ET efficiency of Ru(bpy)<sub>3</sub><sup>2+</sup>-H<sub>2</sub>ase complexes relative to H<sub>2</sub>ase-QD complexes, the likelihood of multiple reduction events from a single Ru(bpy)<sub>3</sub><sup>2+</sup> is very low.

GC analysis of H<sub>2</sub> produced using photosensitization with Ru(bpy)<sub>3</sub><sup>2+</sup> (Figure SI-5) showed a markedly lower solar to hydrogen conversion efficiency of 0.02%. This is likely due to nonspecific binding and possibly preferential electrostatic binding to the large subunit not electronically connected to the active site. No H<sub>2</sub> production was observed without ascorbic acid, H<sub>2</sub>ase, or Ru(bpy)<sub>3</sub><sup>2+</sup>, indicating that each component is obligatory for H<sub>2</sub>ase turnover.

The key differences between the QD- and Ru(bpy)<sub>3</sub><sup>2+</sup>-photodrive enzyme reductions can be summarized as follows: First, QD binding is electrostatic, is screened at high salt concentrations, and quenches QD PL, whereas Ru(bpy)<sub>3</sub><sup>2+</sup> is nonspecifically bound or bound in ET-inactive sites on the enzyme surface, as determined by homology modeling and PL titrations (data not shown). Second, H<sub>2</sub> production with QD-H<sub>2</sub>ase hybrids is reasonably efficient, whereas Ru(bpy)<sub>3</sub><sup>2+</sup> is 100 times less efficient per photon absorbed. Finally, light-induced difference FTIR measurements showed very different populations of intermediate states. Photoreduction with QDs resulted in the formation of the Ni<sub>a</sub>-S state only, whereas Ru(bpy)<sub>3</sub><sup>2+</sup> generated all of the known steady-state intermediates. These are fundamentally different end points in photoreduction, and the Ru(bpy)<sub>3</sub><sup>2+</sup> spectra did not evolve to the QD-H<sub>2</sub>ase spectra at long illumination times. The accumulation of a distribution of intermediates is correlated with inefficient enzyme turnover.

The origins of the differences in the light titration results are not completely understood but certainly have to do with the fundamental differences between Ru(bpy)<sub>3</sub><sup>2+</sup> and QDs. One possible explanation is that the observed differences are purely a consequence of the mode of photosensitizer binding. Homology modeling suggested that positively charged Ru(bpy)<sub>3</sub><sup>2+</sup> may bind nonpreferentially for ET. This non-preferential binding could make the observation of intermediates much more likely since the fundamental reduction events are slower. The mode of binding may also influence the flux of electrons entering the enzyme through the FeS chain versus a more direct route, which in turn could influence the turnover, for example by modulating the efficiency of coupled proton transfers. Finally, QDs may be capable of delivering multiple electrons from multiple photons without requiring hole filling.<sup>28,29</sup> In contrast, Ru(bpy)<sub>3</sub><sup>2+</sup> can deliver only a single electron and then must be regenerated by the SED (no faster than bimolecular diffusion). Thus, QDs may produce multiple reducing equivalents on a time scale that is fast relative to the turnover frequency of the enzyme. This observation raises the possibility that efficient turnover requires fast multielectron reduction and that the partially reduced steady-state intermediates are a consequence of slow single-electron reduction and are not productive. Further experiments will be required to determine the source of the observed differences.

In summary, we have presented direct spectroscopic and chromatographic evidence of efficient QD-photodrive enzyme reduction and H<sub>2</sub> production using an O<sub>2</sub>-tolerant [NiFe] H<sub>2</sub>ase. We have also demonstrated the power of these QD-H<sub>2</sub>ase assemblies for studying very fast and complex redox



chemistry of enzymes using light triggers, which could open up new doors for subturnover temporal spectroscopic resolution. The strikingly different photoreduction behaviors observed for QD- and Ru(bpy)<sub>3</sub><sup>2+</sup>-sensitized H<sub>2</sub>ases are likely due to multiphoton, multielectron pathways in QD assemblies that are not possible in the case of Ru(bpy)<sub>3</sub><sup>2+</sup>. We intend to elucidate further the mechanism of light-driven H<sub>2</sub>ase turnover using time-resolved IR and transient absorbance experiments capable of directly probing the ET rates and catalytic intermediates.

## ■ ASSOCIATED CONTENT

### ■ Supporting Information

Experimental details on homology modeling, QD synthesis, H<sub>2</sub>ase expression and purification, GC calibration, Ru(bpy)<sub>3</sub><sup>2+</sup> photocatalytic H<sub>2</sub> production, anaerobic FTIR light titrations, and explicit efficiency calculations. This material is available free of charge via the Internet at <http://pubs.acs.org>.

## ■ AUTHOR INFORMATION

### Corresponding Author

briandyer@emory.edu

### Notes

The authors declare no competing financial interest.

## ■ ACKNOWLEDGMENTS

This project was funded by the U.S. Army Research Laboratory and the U.S. Army Research Office (Grant 5463SCH) the NIH (Grant GM068036). The authors thank Julius O. Campeciño for protein purification work.

## ■ REFERENCES

- (1) Fisher, H. F.; Krasna, A. I.; Rittenberg, D. *J. Biol. Chem.* **1954**, *209*, 569.
- (2) Ludwig, M.; Cracknell, J. A.; Vincent, K. A.; Armstrong, F. A.; Lenz, O. *J. Biol. Chem.* **2009**, *284*, 465.
- (3) Pandelia, M. E.; Nitschke, W.; Infossi, P.; Giudici-Ortoni, M. T.; Bill, E.; Lubitz, W. *Proc. Natl. Acad. Sci. U.S.A.* **2011**, *108*, 6097.
- (4) Gogotov, I. N.; Zorin, N. A.; Serebriakova, L. T.; Kondratieva, E. N. *Biochim. Biophys. Acta* **1978**, *523*, 335.
- (5) Shomura, Y.; Yoon, K. S.; Nishihara, H.; Higuchi, Y. *Nature* **2011**, *479*, 253.
- (6) Brown, K. A.; Dayal, S.; Ai, X.; Rumbles, G.; King, P. W. *J. Am. Chem. Soc.* **2010**, *132*, 9672.
- (7) Reisner, E.; Powell, D. J.; Cavazza, C.; Fontecilla-Camps, J. C.; Armstrong, F. A. *J. Am. Chem. Soc.* **2009**, *131*, 18457.
- (8) Krassen, H.; Schwarze, A.; Friedrich, B.; Ataka, K.; Lenz, O.; Heberle, J. *ACS Nano* **2009**, *3*, 4055.
- (9) Nedoluzhko, A. I.; Shumilin, I. A.; Nikandrov, V. V. *J. Phys. Chem.* **1996**, *100*, 17544.
- (10) Cuendet, P.; Rao, K. K.; Grätzel, M.; Hall, D. O. *Biochimie* **1986**, *68*, 217.
- (11) Zadovnyy, O. A.; Lucon, J. E.; Gerlach, R.; Zorin, N. A.; Douglas, T.; Elgren, T. E.; Peters, J. W. *J. Inorg. Biochem.* **2012**, *106*, 151.
- (12) Lubner, C. E.; Grimme, R.; Bryant, D. A.; Golbeck, J. H. *Biochemistry* **2010**, *49*, 404.
- (13) Madden, C.; Vaughn, M. D.; Diez-Perez, I.; Brown, K. A.; King, P. W.; Gust, D.; Moore, A. L.; Moore, T. A. *J. Am. Chem. Soc.* **2012**, *134*, 1577.
- (14) Ogata, H.; Kellers, P.; Lubitz, W. *J. Mol. Biol.* **2010**, *402*, 428–444.
- (15) Sali, A.; Blundell, T. L. *J. Mol. Biol.* **1993**, *234*, 779.

- (16) Mattoussi, H.; Mauro, J. M.; Goldman, E. R.; Anderson, G. P.; Sundar, V. C.; Mikulec, F. V.; Bawendi, M. G. *J. Am. Chem. Soc.* **2000**, *122*, 12142.
- (17) Ipe, B. I.; Niemeyer, C. M. *Angew. Chem., Int. Ed.* **2006**, *45*, 504.
- (18) deLacey, A. L.; Hatchikian, E. C.; Volbeda, A.; Frey, M.; Fontecilla-Camps, J. C.; Fernandez, V. M. *J. Am. Chem. Soc.* **1997**, *119*, 7181.
- (19) Bleijlevens, B.; van Broekhuizen, F. A.; De Lacey, A. L.; Roseboom, W.; Fernandez, V. M.; Albracht, S. P. J. *J. Biol. Inorg. Chem.* **2004**, *9*, 743.
- (20) Bagley, K. A.; Duin, E. C.; Roseboom, W.; Albracht, S. P. J.; Woodruff, W. H. *Biochemistry* **1995**, *34*, 5527.
- (21) Jones, A. K.; Lamle, S. E.; Pershad, H. R.; Vincent, K. A.; Albracht, S. P. J.; Armstrong, F. A. *J. Am. Chem. Soc.* **2003**, *125*, 8505.
- (22) Armstrong, F. A.; Albracht, P. J. *Philos. Trans. R. Soc., A* **2005**, *363*, 937.
- (23) Brown, K. A.; Wilker, M. B.; Boehm, M.; Dukovic, G.; King, P. W. *J. Am. Chem. Soc.* **2012**, *134*, 5627.
- (24) Whitehead, J. P.; Gurbel, R. J.; Bagyinka, C.; Hoffman, B. M.; Maroney, M. J. *J. Am. Chem. Soc.* **1993**, *115*, 5629.
- (25) Kellers, P.; Pandelia, M. E.; Currell, L. J.; Gerner, H.; Lubitz, W. *Phys. Chem. Chem. Phys.* **2009**, *11*, 8680.
- (26) Ghosh, P. K.; Brunschwig, B. S.; Chou, M.; Creutz, C.; Sutin, N. *J. Am. Chem. Soc.* **1984**, *106*, 4772.
- (27) Macartney, D. H.; Sutin, N. *Inorg. Chim. Acta* **1983**, *74*, 221.
- (28) Vanhouten, J.; Watts, R. J. *J. Am. Chem. Soc.* **1976**, *98*, 4853.
- (29) Zhu, H.; Song, N.; Rodriguez-Cordoba, W.; Lian, T. *J. Am. Chem. Soc.* **2012**, *134*, 4250.